ISSN Print: 2394-7500
ISSN Online: 2394-5869
Impact Factor: 5.2
IJAR 2017; 3(1): 501-515
www.allresearchjournal.com
Received: 07-11-2016
Accepted: 08-12-2016

JS Rajput
Department of Physical Sciences, M. G. C. G. Vishwavidyalaya, Chitrakoot, Uttar Pradesh, India

V Upadhyay
Department of Physical Sciences, M. G. C. G. Vishwavidyalaya, Chitrakoot, Uttar Pradesh, India

NP Singh
Department of Mathematics, C. L. Jain (PG) College Firozabad, Uttar Pradesh, India

Correspondence
JS Rajput
Department of Physical Sciences, M. G. C. G. Vishwavidyalaya, Chitrakoot, Uttar Pradesh, India

Unsteady hydromagnetic convective flow of micropolar fluid along a semi-infinite vertical porous plate embedded in non-homogeneous porous medium: Analysis with radiation, heat source/sink and variable suction/injection in slip flow regime

JS Rajput, V Upadhyay and NP Singh

Abstract
In the present paper unsteady hydromagnetic convective flow of micropolar fluid along a semi-infinite vertical porous plate is studied with effects of radiation and heat source/sink. The porous plate is embedded in non-homogeneous porous medium and subjected to a variable suction/injection in slip flow regime taking into account the effects of radiation and heat source/sink. The plate is subjected to variable suction/injection in slip flow regime. The suction/injection on the plate and the permeability of the porous medium decreases exponentially with time. Rosseland approximation is used to describe the radiative heat flux. The solutions for the velocity of the fluid, micro-rotation velocity and temperature field are obtained by regular perturbation technique. Expressions for the skin-friction and the rate of heat transfer are also derived. The effects of permeability parameter, couple stress, Prandtl number and other parameters entering into the problem are shown graphically and discussed numerically.

Keywords: Micropolar fluid, radiative heat flux, porous plate, radiation, variable permeability

Nomenclature

A small positive constant,
B_0 uniform magnetic field,
C_p specific heat at constant pressure,
Gr Grashof number,
g acceleration due to gravity,
j' micro-inertia density,
j non-dimensional micro-inertia,
k effective thermal conductivity,
k_c absorption coefficient,
K_0 mean permeability of the medium,
L mean free path,
m_1 Maxwell's reflection coefficient,
n^* dimensional exponential index,
n non-dimensional exponential index,
Pr Prandtl number,
q^* radiative heat flux in y^* –direction,
T^* dimensional temperature of the fluid,
T non-dimensional temperature of the fluid,

T_{∞}^{*} temperature far away from the plate,

T_{w}^{*} temperature of the plate,

t^{*} dimensional time,

t non-dimensional time,

u_0 scale of free stream velocity,

u^{*}, v^{*} dimensional components of velocity along x' and y' -directions,

u, v non-dimensional components of velocity along x' and y' -directions,

v_0 scale of suction velocity,

x^{*}, y^{*} dimensional spatial coordinates along and normal to the plate,

x, y non-dimensional spatial coordinates along and normal to the plate

Greek symbols

α effective thermal diffusivity of the fluid,

β coefficient of volumetric expansion of the fluid,

κ vortex viscosity,

γ specific heat ratio

ε perturbation/reference parameter ($<< 1$),

ρ density of the fluid,

σ electrical conductivity of the fluid,

σ_S Stefan-Boltzmann constant,

λ micro-rotation parameter,

μ dynamic viscosity of the fluid,

υ kinematic viscosity of the fluid,

υ_r kinematic rotational viscosity of the fluid,

ω^{*} dimensional micro-rotation variable,

ω non-dimensional microrotation variable,

γ_1' dimensional spin gradient viscosity,

γ_1 non-dimensional spin gradient velocity.

Introduction

Convective heat transfer in porous medium is gaining interest of the researchers due to its wide range of applications. These applications include insulation of high temperature gas-solid reaction vessels, petroleum reservoir, pollutant dispersion in aquifers, fiber and granular insulation including structures for high power density machines, ceramic radiant porous burners used by industrial firms as efficient heat transfer devises, reduction of hazardous combustion products using catalytic porous beds and solar collectors with absorbers. In the literature on convective heat transfer phenomenon for fluid saturated porous medium, a wealth of information is available and satisfactory means have been evolved for the estimation of the velocity and temperature fields as well as for the drag, heat and mass transfer coefficients involving porous media. Comprehensive literature on the subject is available in the monographs and books of Ene and Polisevski [10], Nakayama [29], Kaviany [20], Nield and Bejan [30] and Vafai [43].

Several authors such as Brinkman [6], Yamamoto and Iwamura [45], Raptis [34], Raptis and Singh [33] and Raptis and Perdikis [32] investigated flow through porous medium and assumed the flow to be governed by generalized Darcy law. In all the above papers generalized Darcy law is derived without taking into account the angular velocity of the fluid particles following Newtonian hypothesis. Due to growing use of Newtonian fluids, considerable efforts have been directed towards the understanding of their flow and heat transfer characteristics. In the literature the fluids with microstructure and asymmetrical stress-tensor are known as micropolar fluids. Physically, they represent fluids consisting of randomly oriented particles suspended in a viscous medium. In fact, a micropolar fluid is one which contains suspensions of rigid particles and exhibits a micro-structure such as blood, liquid crystals, dirty oils, polymers, paints and colloidal fluids. The theory of such fluids was first formulated by Eringen [11], which includes the effect of local rotary inertia, the couple stresses and inertial spin. Eringen [12] also developed the theory of micropolar fluids for the case where only micro-rotational effect and micro-rotational inertia exist. Yucel [46] extended the theory of thermo-micropolar fluids and derived the constitutive laws for fluids with micro-structure. An excellent review of micropolar fluids and their applications was given by Ariman *et al*. [4, 5] Lucaszewicz [27] and Jain and Taneja [17], Taneja and Jain [42] have presented comprehensive literature on micropolar fluids, thermomicropolar fluids and their applications in engineering and technology.

Convective flow of the fluids with micro-structure is an interesting area of research including polymer fluids and fluids with suspensions. In view of the flow through a porous medium in geothermal region, situations may arise when the flow becomes

unsteady, and also the slip at the boundary may take place. In such a situation of slip flow, ordinary continuum approach fails to yield satisfactory results. Recently, Khandelwal and Jain [21, 22], Jain and Gupta [16] have studied problems of micropolar / magneto polar fluid flow through porous medium in slip flow regime. In these problems, the permeability of the porous medium is considered to be constant. However, the permeability of the porous medium is not necessarily constant because the porous material containing the fluid is a non-homogeneous medium. In the light of this fact, Srikanth *et al*. [41] have investigated the effects of permeability variation on free convection flow past a vertical porous wall in a non-homogeneous porous medium, when the permeability varies in time. Recently, Singh *et al*. [38] have discussed hydromagnetic free convection and mass transfer flow of a viscous stratified fluid considering variation in permeability with direction, whereas in another study Singh *et al*. [40] have investigated heat and mass transfer in MHD flow of an incompressible, electrically conducting, viscous fluid past an infinite vertical porous plate embedded in non-homogeneous porous medium of time dependent permeability with oscillatory suction velocity. In these investigations the slip at the boundary is not taken into account. More recently, Jain and Gupta [15], Singh *et al*. [37] and Singh *et al*. [39] have investigated problems with slip flow regime under different physical situations.

In all the above mentioned studies the temperature involved were considered to be moderate. Hence, these studies are limited only to applications where radiative heat transfer is negligible. In fact, many processes in new engineering areas occur at high temperatures, wherein the knowledge of radiation heat transfer becomes very important for the design of the pertinent equipment. Nuclear power plants, gas turbines and the various propulsion devices for aircraft, missiles, satellites and space vehicles are examples of such engineering areas. Perdikis and Raptis [32] studied the heat transfer of a micropolar fluid in the presence of radiation. Raptis [33] studied the effect of radiation on the flow of a micropolar fluid past a continuously moving plate. Recently, Elbarbary and Elgazery [34] used the Chebyshev finite difference method to study the effect of variable viscosity on magneto-micropolar fluid flow with radiation. Moreover, when the radiative heat transfer takes place, the fluid involved can be electrically conducting in the sense that it is ionized owing to the high operating temperature. Accordingly, it is of interest to examine the effect of the magnetic field on the flow. Studying such an effect has a great importance in the application fields, where thermal radiation and magnetohydrodynamics (MHD) are correlative. The process of fusing of metals in an electrical furnace by applying a magnetic field and the process of cooling of the first wall inside a nuclear reactor containment vessel, where the hot plasma is isolated from the wall by applying a magnetic field are examples of such fields. Several investigators have made theoretical and experimental studies of micropolar flow in the presence of a transverse magnetic field during the last three decades (see for example [35-39]). The general theory of magneto-micropolar fluids can be found in [40]. It is important to know that most of the studies on the heat convective flow past a solid surface (whether thermal radiation takes place or not) were restricted, in general, to the case where temperature differences between the plate and the ambient fluid are small. In this case the Boussinesq approximation [41] can be used to treat the fluid density as a constant in the continuity, momentum, angular momentum and heat diffusion equations and treat it as a variable only in the buoyancy term of the momentum equation.

The present paper extends the work of Singh *et al*. [39] to study the effects of radiative convection in the presence of variable permeability and variable suction/injection velocity. Boussinesq approximation is simulated to investigate the effects of different parameters entering into the problem. The fluid velocity, angular velocity, temperature distribution, skin-friction and rate of heat transfer are investigated numerically, shown graphically and discussed. This paper enhances the applications of the work of Singh *et al*. [39] for flows in non-homogeneous porous medium.

Formulation of the Problem

We consider two dimensional, radiative, free convection, unsteady, laminar flow of an electrically conducting, incompressible, micropolar fluid past an infinite porous vertical flat plate embedded in a non-homogeneous porous medium in slip flow regime in the presence of heat source/sink and transversely applied uniform magnetic field. The plate is porous in nature and is subjected to the suction/injection velocity, which decreases exponentially with time about a non-zero constant mean value. In two-dimensional, rectangular cartesian coordinate system, the x^*-axis is chosen along the porous plate, which moves with uniform velocity $u^* = u_0\left(1+\varepsilon e^{-n^* t^*}\right)$ and decreases exponentially with time, the y^*-axis normal to it. In addition, the present analysis is based on the following postulates:

(i) The applied uniform magnetic field is of small magnetic Reynolds number and acts transversely to the direction of the flow.
(ii) Since the magnetic field Reynolds number is small, the induced magnetic field is negligible.
(iii) The Hall effect, the polarization effect, viscous dissipation effect and Ohmic heat effect are ignored.
(iv) To simplify formulation of the boundary conditions, the size of holes in the porous plate is assumed much larger than the characteristic microscopic length scale of the micropolar fluid.
(v) The plate is assumed semi-infinite so that the flow variables are functions of the normal distance y^* and the time t^* only.
(vi) All physical properties of the fluid are constant except variation in density with temperature.
(vii) Boussinesq approximation is invoked, so that density differences are only manifested in the buoyancy terms only.
(viii) The permeability of the porous medium and the suction / injection velocity are assumed to be of the form $K^*(t) = K_0^*\left(1+\varepsilon e^{-n^* t^*}\right)$ and $v^*(t) = -v_0^*\left(1+\varepsilon A e^{-n^* t^*}\right)$ respectively, where A is a real positive constant and $\in$ is small parameter such that $0 < \in A \le 1$.
(ix) The equation of angular momentum is written following Elbarbary and Elgazery [8], Lok *et al*. [26] and Aboeldahab and Azzam [1].

Under the present configuration and assumptions, the equations governing the flow are:
Equation of continuity:

$$\frac{\partial v^*}{\partial y^*} = 0 \quad . \tag{1}$$

The equation (1) implies that v^* is either constant or function of time. Let us assume:

$$v^* = v_0\left(1+\varepsilon A \in e^{-n^* t^*}\right) . \tag{2}$$

Introducing (2) in equation of momentum, angular momentum and energy, these equations are transformed into the following equations:
Equation of momentum:

$$\frac{\partial u^*}{\partial t^*} - v_0\left(1+\varepsilon A e^{-n^* t^*}\right)\frac{\partial u^*}{\partial y^*} = \left(\frac{\mu + K}{\rho}\right)\frac{\partial^2 u^*}{\partial y^{*2}} + g\beta\left(T^* - T_\infty^*\right) - \frac{\upsilon}{K_0^*\left(1+\varepsilon e^{-n^* t^*}\right)}u^* - \frac{\sigma}{\rho}B_0^2 u^* + \frac{K}{\rho}\frac{\partial \omega^*}{\partial y^*} . \tag{3}$$

Equation of angular momentum:

$$\frac{\partial \omega^*}{\partial t^*} - v_0\left(1+\varepsilon A e^{-n^* t^*}\right)\frac{\partial \omega^*}{\partial y^*} = \frac{\gamma_1'}{\rho j'}\frac{\partial^2 \omega^*}{\partial y^{*2}} - \frac{\kappa}{\rho j'}\left(2\omega^* + \frac{\partial u^*}{\partial y^*}\right) . \tag{4}$$

Equation of energy:

$$\frac{\partial T^*}{\partial t^*} - v_0\left(1+\varepsilon e^{-n^* t^*}\right)\frac{\partial T^*}{\partial y^*} = \frac{K_T}{\rho C_p}\frac{\partial^2 T^*}{\partial y^{*2}} - \frac{1}{\rho C_p}\frac{\partial q^*}{\partial y^*} - \frac{Q'}{\rho C_p}\left(T^* - T_\infty^*\right) . \tag{5}$$

The appropriate boundary conditions of the problem for velocity and temperature (see Eckert and Drakey [7]) field are:

$$u^* = u_0\left(1+\varepsilon e^{-n^* t^*}\right) + \frac{(2-m_1)L}{m_1}\frac{\partial u^*}{\partial y^*}, \quad \omega^* = -m\frac{\partial u^*}{\partial y^*}, \quad T^* = T_w^* + \varepsilon\left(T_w^* - T_\infty^*\right)e^{-n^* t^*} + \frac{(2-m_1)}{m_1}\frac{2}{(\gamma+1)}\frac{L}{Pr} \quad \text{at} \quad y = 0 .$$

$$u^* \to 0, \ \omega^* \to 0, \ T^* \to T_\infty^* \ \text{as} \ y^* \to \infty . \tag{6}$$

The symbols are defined in the nomenclature.

By the use of Rosselands approximation (see Warren *et al*. [44]) the radiative heat flux in the y^* –direction is expressed as:

$$q^* = -\frac{4}{3}\frac{\sigma_s}{k_c}\frac{\partial T^{*4}}{\partial y^*} . \tag{7}$$

where σ_s is the Stefan-Boltzmann constant and k_c is the mean absorption coefficient. For sufficient small temperature differences within the flow, the radiative heat flux described in (6) can be linearized by expanding T^{*4}, neglecting higher order terms, into Taylor series about T_∞^* to give $T^{*4} \cong 4T_\infty^{*3}T - 3T_\infty^{*4}$. (8)
It should be noted that by using the Rosseland approximation to describe the radiative heat flux in energy equation, limits our analysis to absorbing-emitting but non-scattering optically thick medium. The microrotation variable ω', which describes its relationship with the surface stress in the relation $\omega' = -m\frac{\partial u'}{\partial y}$, is shown in boundary condition as:

$$\omega^* = -m\frac{\partial u^*}{\partial y^*} . \tag{9}$$

The parameter *m* is the number between 0 and 1 that relates the micro-gyration vector to the shear stress. The value $m = 0$ corresponds to the case, where the particle density is sufficiently large so that microelements close to the wall are unable to rotate. The value $m = 0.5$ is indicative of week concentrations, whereas $n = 1$ represents turbulent boundary layers (see Kim and Fedorov [24], Rees and Bassom [35]).
To solve the equations governing the flow, we introduce the following non-dimensional quantities:

$$u = \frac{u^*}{u_0}, \quad v = \frac{v^*}{v_0}, \quad y = \frac{v_0 y^*}{\upsilon}, \quad t = \frac{t^* v_0^2}{\upsilon}, \quad j = \frac{j' v_0^2}{\upsilon}, \quad \gamma' = \frac{\gamma_1' v_0^2}{\upsilon^2}, \quad n = \frac{n^* \upsilon}{v_0^2}, \quad \omega = \frac{\omega^* \upsilon}{u_0 v_0}, \quad T = \frac{T^* - T_\infty^*}{T_w^* - T_\infty^*}$$

.Introducing above stated non-dimensional quantities in equations (3)-(5), we obtain:

$$\frac{\partial u}{\partial t}-\left(1+\varepsilon Ae^{-nt}\right)\frac{\partial u}{\partial y}=\left(1+\alpha\right)\frac{\partial^2 u}{\partial y^2}+GrT \quad -\frac{1}{K_0\left(1+\varepsilon e^{-nt}\right)}u-M^2u+\alpha\frac{\partial \omega}{\partial y}, \tag{10}$$

$$\frac{\partial \omega}{\partial t}-\left(1+\varepsilon Ae^{-nt}\right)\frac{\partial \omega}{\partial y}=\frac{1}{\lambda}\frac{\partial^2 \omega}{\partial y2}-N\left(2\omega+\frac{\partial u}{\partial y}\right), \tag{11}$$

$$\frac{\partial T}{\partial t}-\left(1+\varepsilon Ae^{-nt}\right)\frac{\partial T}{\partial y}=\frac{1}{R_1Pr}-QT\frac{\partial^2 T}{\partial y^2}, \tag{12}$$

where $\alpha=\frac{\upsilon_\kappa}{\upsilon}$ (Kinematic rotational viscosity parameter), $Gr=\frac{g\beta\upsilon\left(T_w^*-T_\infty^*\right)}{u_0v_0^2}$ (Grashof number), $K_0^*=\frac{K_0\upsilon^2}{v_0^2}$ (Permeability parameter), $M=\frac{B_0}{v_0}\sqrt{\frac{\sigma\upsilon}{\rho}}$ (Magnetic parameter) $\lambda=\frac{\rho j'}{\gamma'}$ (Microrotation parameter), $Pr=\frac{K_T}{\mu C_p}$ (Prandtl number), $R_1=\left(1-\frac{4}{3R+4}\right)$ (Modified radiation parameter), $R=\frac{K_Tk_C}{4\sigma_S T_\infty^{*3}}$ (Radiation parameter), $Q=\frac{Q^*\upsilon}{v_0^2\rho C_p}$ (Heat source/sink parameter), $N=\frac{\kappa}{\rho j'v_0}$ (Kinematic rotational parameter).

The boundary conditions shown in (5) in non-dimensional form become:

$$u=1+\varepsilon e^{-nt}+h_1\frac{\partial u}{\partial y},\ \omega=-m\frac{\partial u}{\partial y},\ T=1+\varepsilon e^{-nt}+h_2\frac{\partial T}{\partial y} \text{ at } y=0.\ u\to 0,\ w\to 0,\ T\to 0 \text{ as } y\to\infty \tag{13}$$

Where

$h_1=\frac{\left(2-m_1\right)Lv_0}{m_1\upsilon}$ (Rarefaction parameter) and $h_2=\frac{2-m_1}{m_1}\frac{2\gamma}{\left(\gamma+1\right)}\frac{L\upsilon_0}{Pr\upsilon}$ (Temperature jump parameter)

Solution of the Problem

To solve the differential equations (10)-(12), we assume the following solution for u,ω and T, where ε is a small quantity, i.e.,

$$u\left(y,t\right)=u_0\left(y\right)+\varepsilon u_1\left(y\right)e^{-nt}+O\left(\varepsilon^2\right),\ w\left(y,t\right)=w_0\left(y\right)+\varepsilon w_1\left(y\right)e^{-nt}+O\left(\varepsilon^2\right),\ T\left(y,t\right)=T_0\left(y\right)+\varepsilon T_1\left(y\right)e^{-nt}+O\left(\varepsilon^2\right). \tag{14}$$

Introducing (14) into the non-dimensional differential equations (10)-(12) and comparing the coefficient of ε^0 and ε^1, neglecting the coefficient of ε^2 and higher powers, we obtain:

$$\left(1+\alpha\right)\frac{d^2u_0}{dt^2}+\frac{du_0}{dy}-M_1u_0=-GrT_0-\alpha\frac{d\omega_0}{dy}. \tag{15}$$

$$\left(1+\alpha\right)\frac{d^2u_1}{dy^2}+\frac{du_1}{dy}-M_2u_1=-GrT_1-\alpha\frac{d\omega_1}{dy}-\frac{du_0}{dy}-\frac{1}{K_0}u_0. \tag{16}$$

$$\frac{d^2\omega_0}{dy^2}+\lambda\left(1-N\right)\frac{d\omega_0}{dy}-2\lambda N\omega_0=0. \tag{17}$$

$$\frac{d^2\omega_1}{dy^2}+\lambda\left(1-N\right)\frac{d\omega_1}{dy}-\lambda\left(2N-n\right)\omega_1=-\lambda A\frac{d\omega_0}{dy}. \tag{18}$$

$$\frac{d^2T_0}{dy^2}+R_1Pr\frac{dT_0}{dy}-QR_1PrT_0=0. \tag{19}$$

$$\frac{d^2T_1}{dy^2}+R_1Pr\frac{dT_1}{dy}-R_1Pr\left(Q-n\right)=-AR_1Pr\frac{dT_0}{dy}. \tag{20}$$

Introducing (14), the boundary conditions (13) transform to the following form:

$u_0 = 1 + h_1 \frac{\partial u_0}{\partial y}$, $u_1 = 1 + h_1 \frac{\partial u_1}{\partial y}$, $\omega_0 = -m \frac{\partial u_0}{\partial y}$, $\omega_1 = -m \frac{\partial u_1}{\partial y}$, $T_0 = 1 + h_2 \frac{\partial T_0}{\partial y}$, $T_1 = 1 + h_2 \frac{\partial T_1}{\partial y}$ at $y = 0$.

$u_0 \to 0$, $u_1 \to 0$, $\omega_0 \to 0$, $\omega_1 \to 0$,

$T_0 \to 0$, $T_1 \to 0$ as $y \to \infty$. (21)

Solutions of differential equations (15)-(20) satisfying boundary conditions (21) are obtained as follows:

$$\omega_0 = C_1 e^{-m_1 y}. \quad (22)$$

$$\omega_1 = C_2 e^{-m_2 y}. \quad (23)$$

$$T_0 = C_3 e^{-m_3 y}. \quad (24)$$

$$T_1 = C_4 e^{-m_4 y} + K_2 e^{-m_3 y}. \quad (25)$$

$$u_0 = C_5 e^{-m_5 y} - K_3 e^{-m_3 y} + K_4 e^{-m_1 y}. \quad (26)$$

$$u_1 = C_6 e^{-m_6 y} + K_5 e^{-m_1 y} + K_6 e^{-m_2 y} + K_7 e^{-m_3 y} - K_8 e^{-m_4 y} + K_9 e^{-m_5 y}. \quad (27)$$

The constant are defined in appendix.

Skin-Friction and Rate of Heat Transfer

The non-dimensional skin-friction (τ) at the plate is given by:

$$\tau = (1+\alpha)\left(\frac{\partial u}{\partial y}\right)_{y=0} = (1+\alpha)\left(\frac{\partial u_0}{\partial y}\right)_{y=0} + \varepsilon(1+\alpha)\left(\frac{\partial u_1}{\partial y}\right)_{y=0} e^{-nt} = P_1 + \in P_2 e^{-nt}. \quad (28)$$

The non-dimensional rate of heat transfer in terms of Nusselt number (*Nu*) is given by:

$$Nu = \left(\frac{\partial T}{\partial y}\right)_{y=0} = \left(\frac{\partial T_0}{\partial y}\right)_{y=0} + \varepsilon\left(\frac{\partial T_1}{\partial y}\right)_{y=0} e^{-nt} = -m_3 C_3 + \in \left(-m_4 C_4 - m_3 K_3\right) e^{-nt}. \quad (29)$$

Results and Discussion

Unsteady radiative convection flow of micropolar fluid along a semi-infinite vertical porous plate embedded in non-homogeneous porous medium with variable suction is investigated in the presence of heat source/sink. The solutions for the microrotation velocity (ω), temperature (T) and the velocity (u) are obtained and expressed in (22)-(27). In order to obtain physical insight into the problem and establish the effects of different parameters on the microrotation velocity, the flow field and the temperature distribution; numerical calculations are performed and presented graphically. These figures show that the stream-wise velocity and micro-rotation as well as temperature profiles for the micropolar fluid with the fixed flow conditions $\varepsilon = 0.02$, $n = 0.1$, $A = 1.0$, $K_0 = 5.0$ and $t = 1.0$, whereas Grashof number (*Gr*), Prandtl number (*Pr*), magnetic parameter (*M*), heat source/sink (*Q*), slip flow parameter (h_1), temperature jump parameter (h_2) and viscosity ratio (α) are varied over a range which are listed in caption of the figures. To be realistic, the values of Prandtl number (*Pr*) are chosen for air $Pr = 0.71$, electrolyte solutions ($Pr = 1.0$) and water ($Pr = 7.0$). Also, the values of Grashof number (*Gr*) are chosen for cooling of the porous plate ($Gr > 0$) due to practical applications in nuclear technology and geophysical energy systems. The values of the remaining parameters are chosen arbitrarily or following Kim and Fedorov [24].

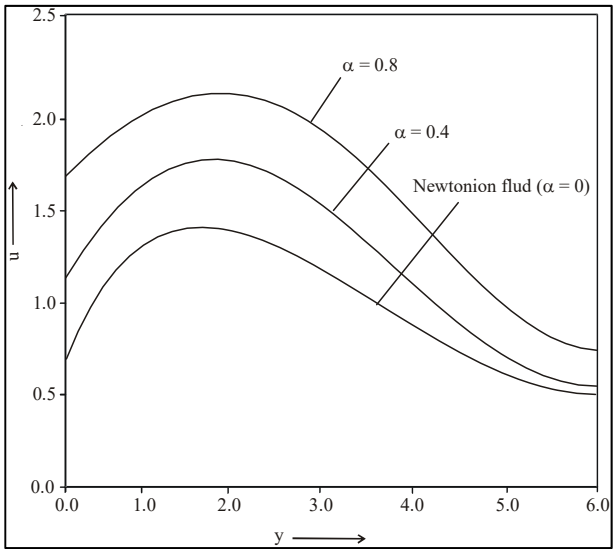

Fig 1: Variation in velocity profile against y for different values of α at n = 0.1, t = 1.0, ε = 0.02, K_0 = 5.0, m = 0.1, N = 0.5, Q = 5.0, h_1 = 0.2, h_2 = 0.5, Pr = 1.0, λ = 0.2, M = 0.5, R = 1.0 and Gr = 5.0.

Figure 1 is intended to illustrate the variations in velocity profiles against *y* for different numerical values of kinematic rotational viscosity parameter (α) at the fixed values of $n = 0.1$, $t = 1.0$, $\varepsilon = 0.02$, $K_0 = 5.0$, $m = 0.1$, $N = 0.5$, $Q = 5.0$, $h_1 = 0.2$, $h_2 = 0.5$, $Pr = 1.0$, $\lambda = 0.2$, $M = 0.5$, $R = 1.0$ and $Gr = 5.0$. It is observed that the velocity field increases with increase in kinematic rotational viscosity parameter. From the velocity profiles, we conclude that the velocity is less for the Newtonian fluid ($\alpha = 0$) with the same flow conditions and fluid properties, compared to the micropolar fluid. When the kinematic rotational viscosity parameter is less than 1.0, the velocity increases in the vicinity of the plate and after attaining a peak value it decreases smoothly with increase in *y*. However, when α takes values greater than 1.0, i.e., the gyro-viscosity is larger than the translational viscosity, the velocity distribution shows a decelerating nature near the porous plate. This conclusion is in agreement to that obtained by Jain and Gupta [16].

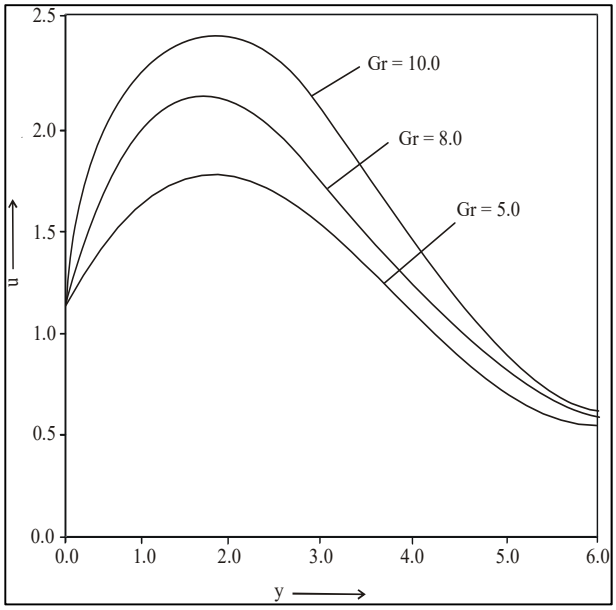

Fig 2: Variation in velocity profile against y for different values of Gr at n = 0.1, t = 1.0, ε=0.02, K_0 = 5.0, m = 0.1, N = 0.5, Q = 5.0, h_1 = 0.2, h_2 = 0.5, Pr = 1.0, λ = 0.2, M = 0.5, R = 1.0 and α = 0.4.

Figure 2 shows variations in the velocity profiles versus *y* for different numerical values of Grash of number (*Gr*), for the cooling case ($Gr > 0$) of the moving plate at the fixed values of $n = 0.1$, $t = 1.0$, $\alpha = 0.4$, $\varepsilon = 0.02$, $K_0 = 5.0$, $m = 0.1$, $N = 0.5$, $Q = 5.0$, $h_1 = 0.2$, $h_2 = 0.5$, $Pr = 1.0$, $\lambda = 0.2$, $R = 1.0$ and $M = 0.5$. It is observed that an increase in buoyancy force (*Gr*), leads to a rise in the velocity. Besides, the curves show that the velocity increases rapidly near the porous wall as *Gr* increases and after attaining peak position, it decreases smoothly and tends to be asymptotic as *y* coordinate increases.

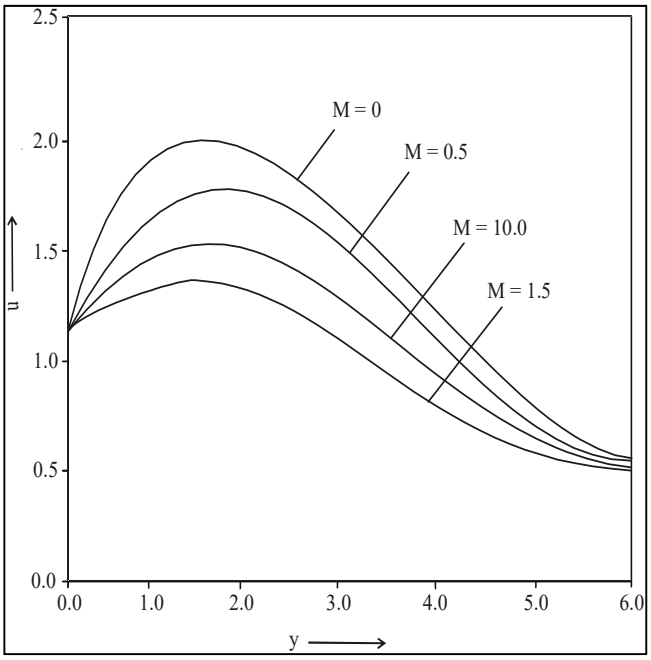

Figure 3 Variation in velocity profile against y for different values of M at n = 0.1, t = 1.0, ε=0.02, K_0 = 5.0, m = 0.1, N = 0.5, Q = 5.0, h_1 = 0.2, h_2 = 0.5, Pr = 1.0, λ = 0.2, α = 0.4, R = 1.0 and Gr = 5.0.

Figure 3 illustrates variations in the velocity profiles against *y* for different numerical values of magnetic field parameter (*M*) at fixed values of $n = 0.1$, $t = 1.0$, $\alpha = 0.4$, $\varepsilon = 0.02$, $K_0 = 5.0$, $m = 0.1$, $N = 0.5$, $Q = 5.0$, $h_1 = 0.2$, $h_2 = 0.5$, $Pr = 1.0$, $\lambda = 0.2$, $R = 1.0$ and $Gr = 5.0$. It is observed that an increase in magnetic field (*M*) decreases velocity distribution across the boundary layer and decays smoothly towards the *y*-axis. In fact, the presence of transverse magnetic field develops a resistive force (Lorentz force), which reduces the velocity.

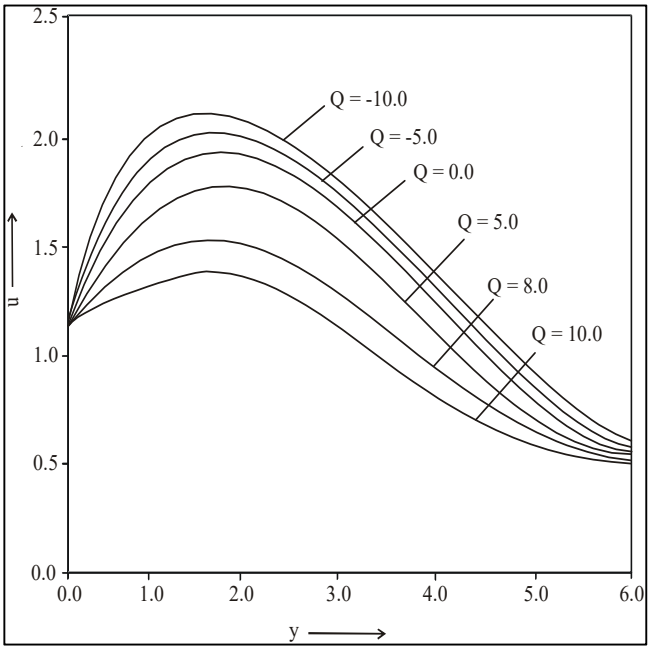

Fig 4: Variation in velocity profile against y for different values of Q at n = 0.1, t = 1.0, ε = 0.02, K_0 = 5.0, m = 0.1, N = 0.5, M = 0.5, h_1 = 0.2, h_2 = 0.5, Pr = 1.0, λ = 0.2, α =0.4, R = 1.0 and Gr = 5.0.

Figure 4 illustrates variations in the velocity profiles against *y* for different values of heat source/sink parameter (*Q*) at fixed values $n = 0.1$, $t = 1.0$, $\varepsilon = 0.02$, $K_0 = 5.0$, $m = 0.1$, $N = 0.5$, $h_1 = 0.2$, $h_2 = 0.5$, $\lambda = 0.2$, $M = 0.5$, $Gr = 5.0$, $\alpha = 0.2$, $R = 1.0$ and $Pr = 1.0$. It is observed that an increase in heat source (negative values of *Q*) increase the velocity, whereas increase in heat sink (positive values of *Q*) decreases the velocity. In fact, heat source reduces the frictional force, which increases the velocity but heat sink increases the frictional force, which decreases the velocity.

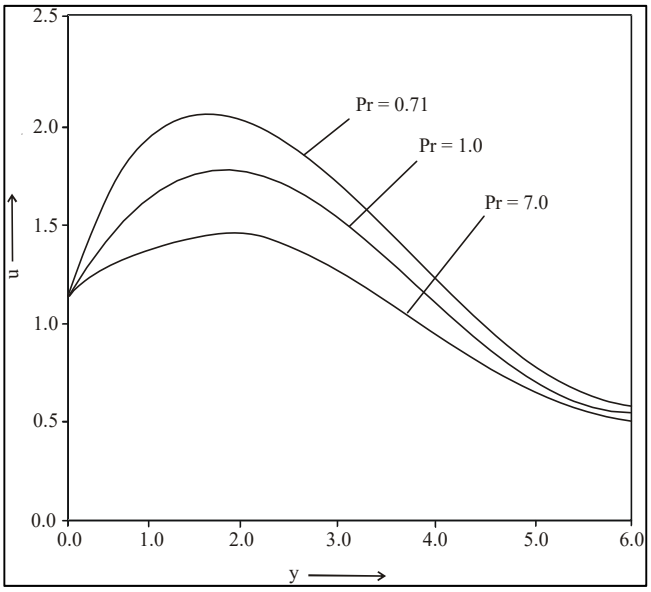

Figure 5 Variation in velocity profile against y for different values of Pr at n = 0.1, t = 1.0, ε = 0.02, K_0 = 5.0, m = 0.1, N = 0.5, M = 0.5, h_1 = 0.2, h_2 = 0.5, Q = 5.0, λ = 0.2, α = 0.4, R = 1.0 and Gr = 5.0.

Figure 5 shows variations in the velocity profiles against span wise coordinate *y* for different values of Prandtl number (*Pr*) at the fixed values $n = 0.1$, $t = 1.0$, $\varepsilon = 0.02$, $K_0 = 5.0$, $m = 0.1$, $N = 0.5$, $Q = 5.0$, $h_1 = 0.2$, $h_2 = 0.5$, $\lambda = 0.2$, $M = 0.5$, $Gr = 5.0$ and $\alpha = 0.2$. It is observed that an increase in Prandtl number (*Pr*) decreases the velocity, which implies that the fluids with lower *Pr* values are favorable to sustain decay in the velocity distribution. In fact, in the light of the definition of Prandtl number, higher *Pr*-values fluid transfer heat less effectively as compared to the lower *Pr*- value fluids. Therefore, the denseness of the fluid particles is more for higher *Pr*-value fluids, so that the velocity decreases with increase in Prandtl number.

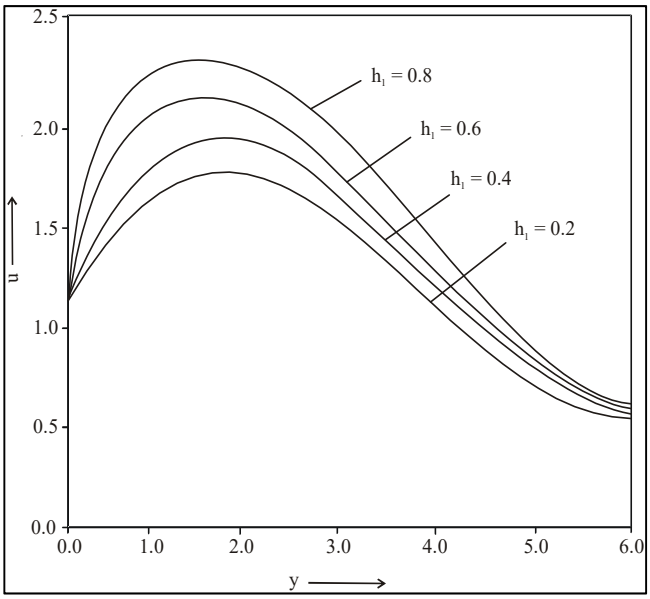

Figure 6 Variation in velocity profile against y for different values of h_1 at n = 0.1, t = 1.0, ε = 0.02, K_0 = 5.0, m = 0.1, N = 0.5, M = 0.5, Pr = 1.0, h_2 = 0.5, Q = 5.0, λ = 0.2, α = 0.4, R = 1.0 and Gr= 5.0.

Figure 6 shows variations in the velocity profiles against *y* for different values of slip flow parameter (h_1) with fixed values of $n = 0.1$, $t = 1.0$, $\varepsilon = 0.02$, $K_0 = 5.0$, $m = 0.1$, $N = 0.5$, $Q = 5.0$, $h_2 = 0.5$, $Pr = 1.0$, $\lambda = 0.2$, $M = 0.5$, $Gr = 5.0$ and $\alpha = 0.4$. It is observed that an increase in h_1 increases the velocity because increase in h_1 reduces the shear-stress at the porous plate, which enhances the velocity. This conclusion is in agreement to that obtained by Khandewal and Jain [22].

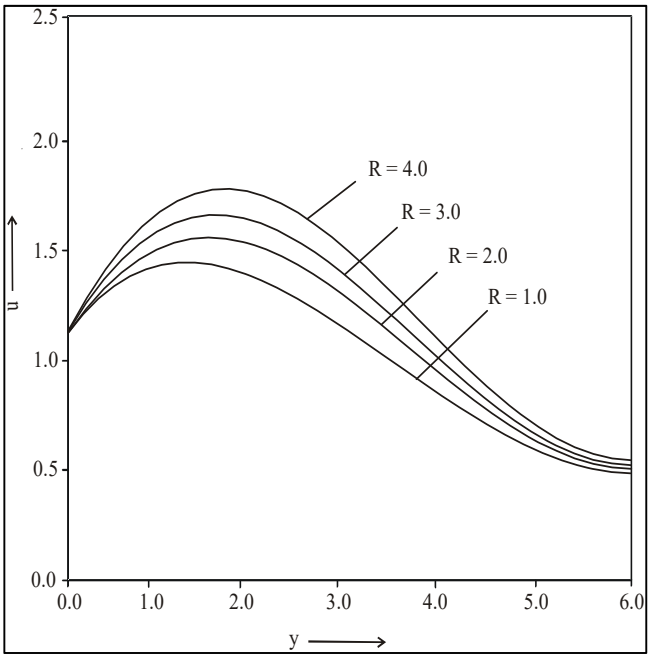

Fig 7: Variations in velocity profiles for different values of R at n = 0.1, t = 1.0, ε = 0.02, K_0 = 5.0, m = 0.1, N = 0.5, M = 0.5, Pr = 1.0, h_2 = 0.5, Q = 5.0, λ = 0.2, α = 0.4, h_1 = 0.2 and Gr = 5.0.

Figure 7 illustrates variations in the velocity profiles against *y* for different values of radiation parameter (*R*) with fixed values of the material parameters. It is observed that an increase in radiation parameter decreases the velocity field because an increase in radiation parameter increases the frictional force between the fluid layers.

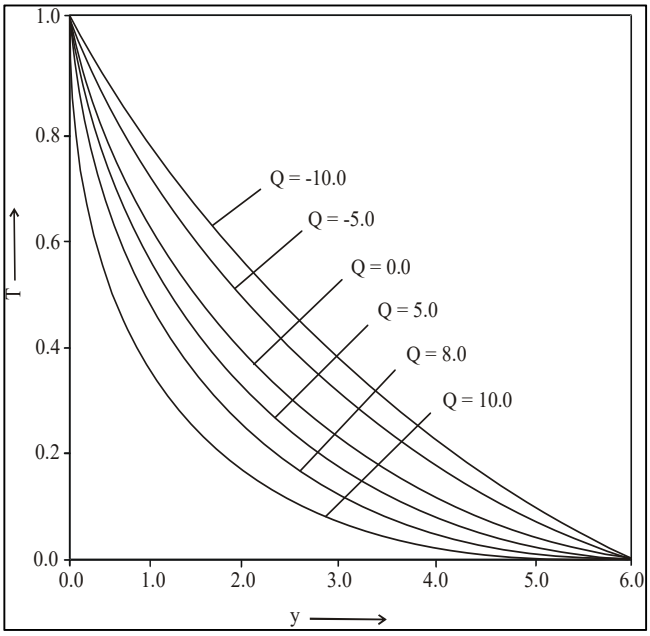

Fig 8: Variations in temperature profiles against y for different values of Q at n = 0.1, t = 1.0, ε = 0.02, h_2 = 0.5, R = 1.0 and Pr = 1.0

Figure 8 is intended to show the variations in temperature profiles with respect to *y* for different values of heat source/sink parameter (*Q*) at fixed values $\varepsilon = 0.02$, $n = 0.1$, $t = 1.0$, $h_2 = 0.5$, $R = 1.0$ and $Pr = 1.0$. As expected, it is observed that an increase in heat source parameter (*Q*) increases the temperature, whereas in increase in heat sink parameter decreases the temperature due to heat generation and heat absorption respectively.

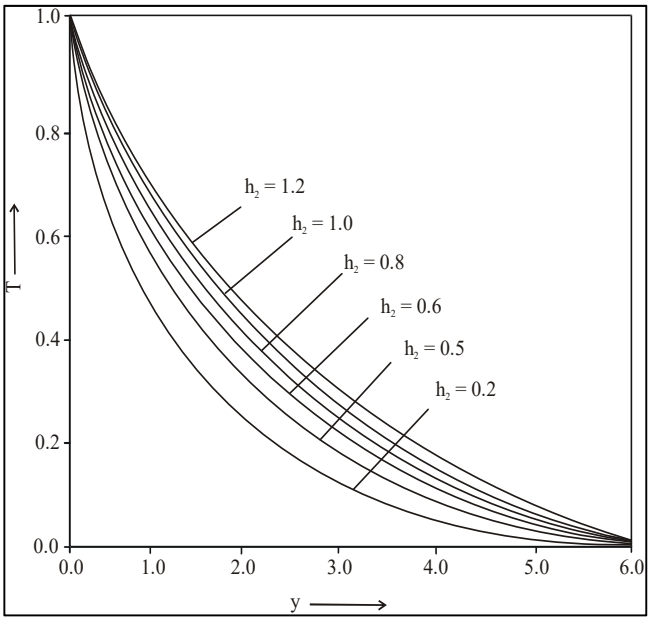

Fig 9: Variations in temperature profiles against y for different values of h_2 at n = 0.1, t = 1.0, ε = 0.02, Q = 5.0, R = 1.0 and Pr = 1.0.

Figure 9 illustrates variations in the temperature distribution versus *y* due to change in the temperature jump parameter (h_2) at fixed values of $\varepsilon = 0.02$, $n = 0.1$, $t = 1.0$, $Q = 5.0$, $R = 1.0$ and $Pr = 1.0$. It is observed that an increase in temperature jump parameter (h_2) increases the temperature field with given flow conditions and material parameters. In fact, an increase in temperature jump parameter results in an increase in thermal boundary layer thickness, so that temperature increases with increase in temperature jump parameter.

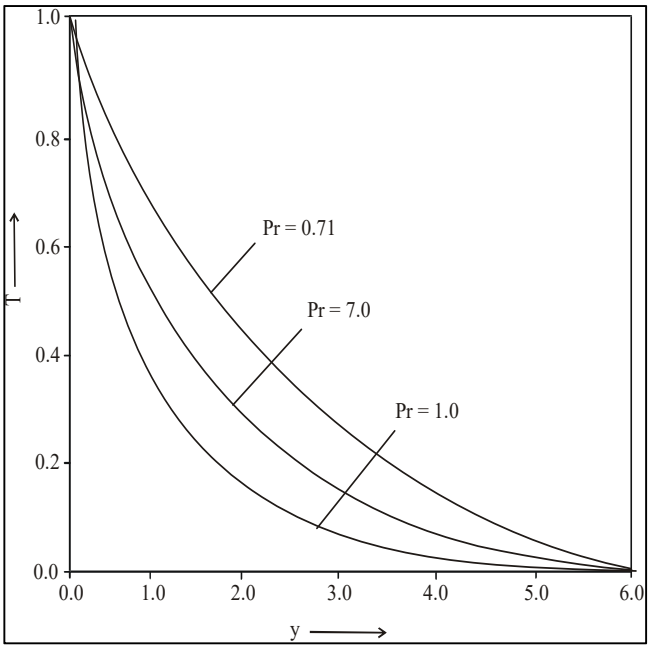

Fig 10: Variations in temperature profiles versus y for different values of Pr at n = 0.1, t = 1.0, ε = 0.02, Q = 5.0, R = 1.0 and h_2 = 0.5.

Figure 10 illustrates the variations in temperature profiles versus *y* for different values of Prandtl number (*Pr*) at fixed values of $\varepsilon = 0.02$, $n = 0.1$, $t = 1.0$, $Q = 5.0$, $R = 1.0$ and $h_2 = 0.5$. It is observed that an increase in Prandtl number, leads to a decrease in temperature, which implies a decrease in thermal boundary layer thickness. This result explains the fact that smaller values of *Pr* are equivalent to increasing the thermal conductivities; so that heat is able to diffuse away from the surface more rapidly than for higher value of *Pr* fluids. Hence, decay in temperature is much sustained in lower *Pr*-value fluids as compared to higher *Pr*-value fluids. This result is in agreement with those of Khandelwal and Jain [21].

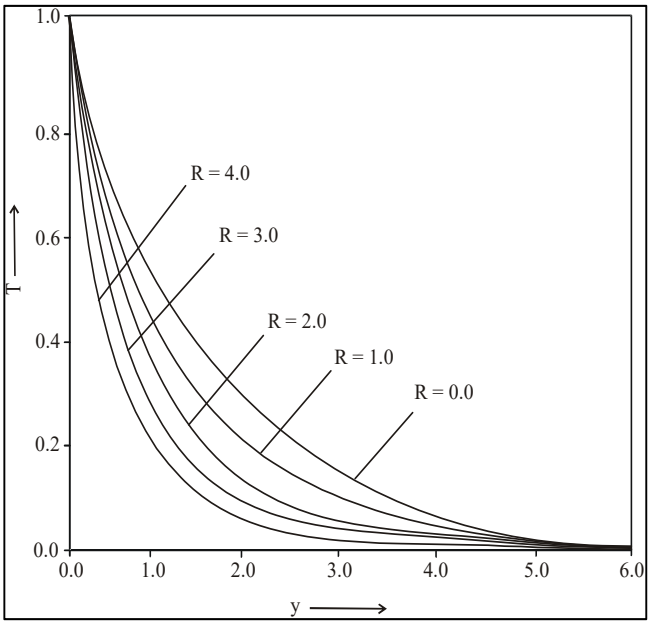

Fig 11: Variations in temperature profiles against y for different values of R at n = 0.1, t = 1.0, ε = 0.02, Q = 5.0, Pr = 1.0 and h_2 = 0.5.

Figure 11 shows variations in the temperature distribution with respect to *y* for different values of the radiation parameter (*R*) at fixed values of $\varepsilon = 0.02$, $n = 0.1$, $t = 1.0$, $Q = 5.0$, $h_2 = 0.5$, and $Pr = 1.0$. It is noted that an increase in radiation parameter decreases the temperature field because increase in *R* decreases the thermal boundary layer.

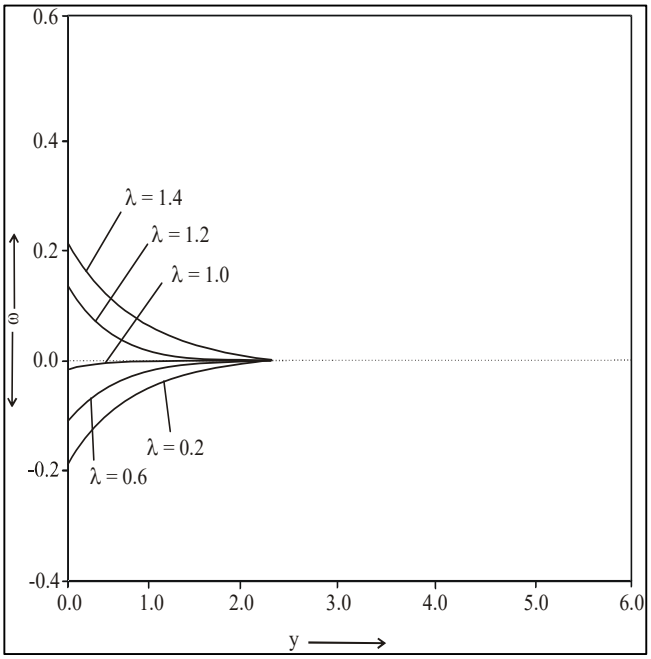

Fig 12 Variations in micro-rotation velocity (ω) for different values of λ at n = 0.1, t = 1.0, ε = 0.02, Q = 5.0, R = 1.0, h_1 = 0.2, h_2 = 0.5, K_0 = 5.0, m = 0.1, M = 0.5, N = 0.5, Gr = 5.0, α = 0.2 and Pr = 1.0.

Figure 12 describes the effect of micro-rotation parameter (λ) on the microrotation velocity (ω) versus *y* for fixed captioned values. It is observed that the microrotation velocity is minimum for laminar flow of Newtonian fluid ($\lambda = 0$) for the same fixed values of the material parameters. As the value of λ increases, the microrotation velocity increases near the plate and becomes asymptotic to *y*-axis as *y* increases. However, for $\lambda > 1$, the microrotation velocity changes its nature and decreases in the vicinity of the plate and shows asymptotic nature towards *y*-axis with increase in *y*-coordinate.

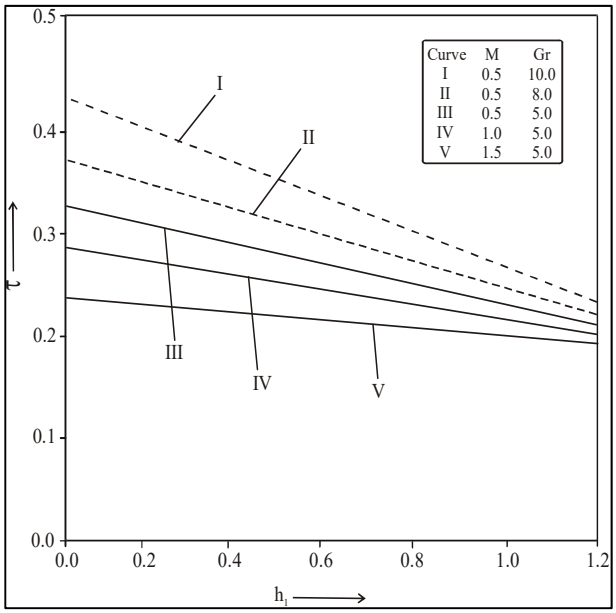

Fig 13: Variations in surface skin-fraction against h_1 for different values of M and Gr at n=0.1, t = 1.0, ε = 0.02, Q = 5.0, R = 1.0, λ= 0.2, h_2 = 0.5, K_0 = 5.0, m = 0.1, N = 0.5, α = 0.4 and Pr = 1.0.

Figure 13 represents variations of the surface skin-friction versus slip velocity parameter (h_1) for various values of magnetic parameter (*M*) and buoyancy parameter (*Gr*). It is observed that for an increase in magnetic parameter (*M*) with given flow conditions and material parameters, leads to an increase surface skin-friction (τ) on the porous plate, whereas an increase in buoyancy parameter (*Gr*) leads to a decrease in surface skin-friction (τ) on the porous plate.

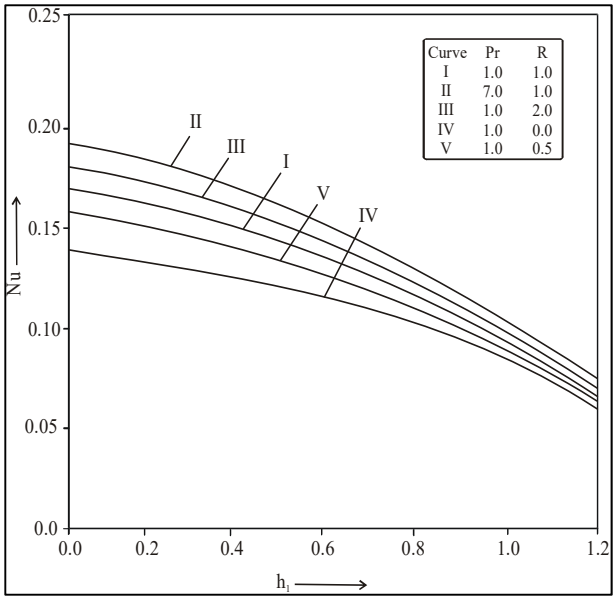

Fig 14: Variations in surface heat transfer against h_2 for different values of Pr and R at n=0.1, t = 1.0, ε = 0.02 and Q = 5.0.

Figure 14 illustrates the variation of surface heat transfer versus temperature jump parameter (h_2) for different values of Prandtl number (*Pr*) and radiation parameter (*R*). It is observed that, as *Pr* is increased or *Gr* increased, the surface heat transfer increases. Moreover, the numerical results show that for the given flow conditions and material parameters, the surface heat transfer from the porous plate tends to decrease slightly on increasing the magnitude of temperature jump parameter.

Conclusions

The problem of velocity slip and temperature jump parameter on unsteady convective flow of a micropolar fluid along a uniformly moving vertical porous plate with time dependent suction velocity, radiation, heat source/sink and non-homogeneous porous medium is investigated. Main conclusions of the study (*Gr* > 0) are as follows:

- The velocity (*u*) increases rapidly near the plate and after attaining peak value it decreases monotonically.

- The velocity (u) increases with increase in Grashof number (Gr), kinematical viscosity parameter (α) or heat source/sink ($Q < 0$) slip flow parameter (h_1) but decreases as magnetic parameter (M), Prandtl number (Pr) radiation parameter (R) or heat sink parameter ($Q > 0$).
- The temperature (T) decreases with increase in Prandtl number (Pr), radiation parameter (R) or heat sink parameter ($Q > 0$) but increases with increase in temperature jump parameter (h_2) or heat source parameter ($Q < 0$).
- The microrotation velocity (ω) increases with increase in microrotation parameter (λ) and changes its nature when λ exceeds the numerical value unity.
- Increasing values of slip velocity parameter (h_1) or buoyancy parameter (Gr) lead to decreasing skin-friction on the porous plate but reverse effect is noted for increasing magnetic induction.
- The heat transfer rate (Nu) increases with increase in Prandtl number (Pr) or radiation parameter (R) but decreases with increase in temperature jump parameter.

References

1. Aboeldahab EM, Azzam GEDA. Unsteady three-dimensional combined heat and mass free convection flow over a stretching surface with time dependent chemical reaction. Acta Mechanica. 2006; 184:121-136.
2. Abo-Eldahab EM, El-Aziz MA. Hall current and Ohmic heating effects on mixed convection boundary layer flow of a micropolar fluid from a rotating cone with power law variation in surface temperature. Int Commun Heat Mass Transfer. 2004; 31:751-762.
3. Abo-Eldahab EM, El-Aziz MA. Flow and heat transfer in a micropolar fluid past a stretching surface embedded in a non-Darcian porous medium with uniform free stream. Appl Math Comp. 2005; 162:881-899.
4. Ariman T, Turk MA, Sylvester ND. Microcontinuum fluid mechanics-A review. Int J Engng Sci. 1973; 11:905-930.
5. Ariman T, Turk MA, Sylvester ND. Applications of microcontinuum fluid mechanics. Int J Engng Sci. 1974; 12:273-293.
6. Brinkman HC. On the permeability of media consisting closely packed porous particles. Appl Sci Res A1:81-81.
7. Eckert ERG, Drake RM. Analysis Heat and Mass Transfer. McGraw-Hill Book Co., New York, 1972, 486.
8. Elbarbary EME, Elgazery NS. Chebyshev finite difference method for the effect of variable viscosity and variable thermal conductivity on heat transfer from moving surfaces with radiation. Int J Thermal Sci. 2004; 43:889-899.
9. Elbarbary ME, Elgazery S. Chebyshev finite difference method for the effect of variable viscosity on magneto-micropolar fluid flow with radiation. Int Commun Heat Mass Transfer. 2004; 31:409-419.
10. Ene HI, Polisevski D. Thermal Flow in Porous Media. D. Reidel, Dordrecht, The Netherlands, 1987.
11. Eringen AC. Theory of Micropolar Fluids. J Math Mech. 1966; 16:1-18.
12. Eringen AC. Theory of Micropolar Fluids. J Math Mech. 1972; 38:480-496.
13. Eringen AC. Micro-continuum Field Theories II: Fluent Media. Springer, New York, 2001.
14. Gorla RSR, Takhar HS, Slaouti A. Magnetohydrodynamic free convection boundary layer flow of a thermomicropolar fluid over a vertical plate. Int J Engng Sci. 1998; 36:315-327.
15. Jain NC, Gupta P. Unsteady hydromagnetic thermal boundary layer flow past an infinite porous surface in slip flow regime. Ganita. 2005; 56:15-25.
16. Jain NC, Gupta Poonam. Unsteady magnetopolar flow past an infinite porous plate with variable suction / injection and variable permeability. Ind J Theo Phys. 2006; 54:129-137.
17. Jain NC, Taneja R. Hydromagnetic flow with time depended suction in slip flow regime. Ganita. 2002; 53:13-21.
18. Kakac S, Yenar Y. Convective Heat Transfer. Hemisphere Publishing Crop. Washington, DC, 1984, 380-381.
19. Kasivishwanathan SR, Gandhi MV. A class of exact solutions for the magnetohydrodynamic flow of a micropolar fluid. Int J Engng Sci. 1992; 30:409-117.
20. Kaviany M. Principals of Heat Transfer in porous Media. 2nd Edition, Springer, New York, 1995.
21. Khandelwal AK, Jain NC. Effect of couple stress on the flow through a porous medium with variable permeability in slip flow regime. Ganita. 2003; 54:203-212.
22. Khandelwal AK, Jain NC. Unsteady magnetopolar free convection flow with variable permeability in slip flow regime. Ganita Sandesh. 2003; 17:1-12.
23. Khandelwal AK, Jain NC. Effects of slip parameters on unsteady MHD free convection mass transfer flow through porous medium of variable permeability with radiation. Ganita. 2006; 57:11-20.
24. Kim YJ, Fedorov AG. Transient mixed radiative convection flow of a micropolar fluid past a moving semi-infinite vertical porous plate. Int J Heat Mass Transfer. 2003; 46:1751-1758.
25. Kumar H, Tak SS. Free convection flow of an unsteady magneto-polar fluid with viscous dissipation and temperature depended heat source in slip flow regime. Acta Cienica Indica. 2007; 33:1043-1055.
26. Lok YY, Amin N, Pop I. Unsteady mixed convection flow of a micropolar fluid near the stagnation point on a vertical surface. Int. J. Thermal Sci. 2006; 45:1149-1157.
27. Lucaszewicz G. Micropolar Fluid Theory and Applications. Birkhauser, Boston, 1999.
28. Mohammadein AA, Gorla RSR. Effects of transverse magnetic field on mixed convection in a micropolar fluid on a horizontal plate with vectored mass transfer. Acta Mech. 1996; 118:1-12.
29. Nakayama A. PC-Aided Numerical Heat Transfer and Convective Flow. CRC Press, Tokyo, 1995.
30. Nield DA, Bejan A. Convection in Porous Media. 3rd Edition Springer, New York, 2006.
31. Perdisik C, Raptis A. Heat transfer of a micropolar fluid by the presence of radiation. Heat Mass Transfer. 1996; 31:381-382.

32. Raptis A, Perdikis CP. Oscillatory flow through a porous medium by the presence of free convective flow. Int J Engng Sci. 1985; 23:51-55.
33. Raptis A, Singh AK. Free convection flow past an impulsively started vertical plate in a porous medium by finite difference method. Astrophys Space Sci. 1985; 112:259-265.
34. Raptis A. Flow of a micropolar fluid past a continuously moving plate by the presence of radiation. Int J Heat Mass Transfer. 1998; 41:2865-2866.
35. Rees DAS, Bassom AP. The Blasius boundary layer flow of a micropolar fluid. Int J Engng Sci. 1996; 34:113-124.
36. Reptis A. Free convective flow through a porous medium bounded by an infinite vertical plate with oscillatory plate temperature and constant suction. Int J Engng Sci. 1983; 21:345-354.
37. Singh Ajay Kumar, Singh Atul Kumar, Singh NP. Heat and mass transfer in MHD flow of a viscous fluid past a vertical plate under oscillatory suction velocity. Int J Pure Appl Math. 2003; 34:429-442.
38. Singh NP, Singh Ajay Kumar, Yadav MK, Singh Atul Kumar. Hydromagnetic free convection and mass transfer flow of a viscous stratified fluid. J Energy Heat Mass Transfer. 1999; 21:111-115.
39. Singh NP, Singh Atul Kumar, Singh Hukum. Unsteady MHD flow with heat and mass transfer through porous medium past an oscillating porous horizontal plate in slip flow regime. Ultra Science. 2008; 20:713-722.
40. Singh NP, Singh Atul Kumar, Singh Hukum. Free convective flow of magnetopolar fluid past a porous vertical wall embedded in non-homogeneous porous medium in slip flow regime. Int J Fluid Mech Res. 2009; 36:357-374.
41. Srikanth S, Venkataramana S, Ramakrishna S. Hydromagnetic free convective flow through a porous medium with variable permeability. Acta Ciencia Indica. 1996; 22:267-275.
42. Taneja R, Jain NC. Effects of magnetic field on free convection mass transfer flow through porous medium with radiation and variable permeability in slip flow regime. Jnanabha. 2002; 31/32:69-78.
43. Vafai K. Hand Book of Porous Media. 2nd Edition, Taylor and Francis, New York, 2005.
44. Warren MR, James PH, Young IC. Hand Book of Heat Transfer. McGraw-Hill, 3rd Edition New York Chap. 1998; 7:21-23.
45. Yamamoto K, Iwamura N. Flow with convective acceleration through a porous medium. J Engng Math.1976; 10:41-54.
46. Yucel A. Mixed convection in micropolar fluid flow over a horizontal plate with surface mass transfer. Int J Engng Sci. 1989; 27:1593-1606.

Appendix

$$m_1=\frac{\lambda(1-N)+\sqrt{\lambda^2(1-N)^2+8N\lambda}}{2},\quad m_2=\frac{\lambda(1-N)+\sqrt{\lambda^2(1-N)^2+4\lambda(2N-n)}}{2},\quad m_3=\frac{R_1Pr+\sqrt{R_1^2Pr^2+8QR_1Pr}}{2},$$

$$m_4=\frac{R_1Pr+\sqrt{R_1^2Pr^2+8R_1Pr(Q-n)}}{2},\quad m_5=\frac{1+\sqrt{1+4(1+\alpha)M_1}}{2},\quad m_6=\frac{1+\sqrt{1+4(1+\alpha)M_2}}{2},$$

$$K_1=\frac{A\lambda m_1C_1}{m_1^2-\lambda(1-N)m_1-\lambda(2N-n)},\quad K_2=\frac{AR_1Pr\,m_3C_3}{m_3^2-R_1Pr\,m_3-R_1Pr(Q-n)},\quad K_3=\frac{GrC_3}{(1+\alpha)m_3^3-m_3-M_1},$$

$$K_4=\frac{\alpha m_1C_1}{(1+\alpha)m_1^2-m_1-M_1},\quad K_5=\frac{K_4\left(Am_1-K_0^{-1}\right)}{(1+\alpha)m_1^2-m_1-M_2},\quad K_6=\frac{\alpha m_2C_2}{(1+\alpha)m_2^2-m_2-M_2},\quad K_7=\frac{K_3\left(K_0^{-1}-Am_3-Gr\right)}{(1+\alpha)m_3^2-m_3-M_2},$$

$$K_8=\frac{GrC_4}{(1+\alpha)m_4^2-m_4-M_2},\quad K_9=\frac{C_5\left(Am_5-K_0^{-1}\right)}{(1+\alpha)m_5^2-m_5-M_2},\quad C_1=\frac{m(m_5L_1-L_2)}{1+h_1m_5},\quad C_2=\frac{m\left[m_6(L_3-L_4)+(1+h_1m_6)L_5\right]}{1+h_1m_6},$$

$$C_3=\frac{1}{1+h_2m_3},\quad C_4=\frac{1-K_2(1+h_2m_3)}{1+h_2m_4},\quad C_5=\frac{1+K_3(1+h_1m_3)-K_4(1+h_1m_1)}{1+h_1m_5},\quad C_6=\frac{L_3-L_4}{1+h_1m_6},$$

$$L_1=1+K_3(1+h_1m_3)-K_4(1+h_1m_3),$$

$$L_2=(K_3m_3-K_4m_1)(1+h_1m_5),\quad L_3=1-K_5(1+h_1m_1)-K_6(1+h_1m_2),$$

$$L_4=K_7(1+h_1m_3)-K_8(1+h_1m_4)+K_9(1+h_1m_5),$$

$$L_5=K_5m_1+K_6m_2+K_7m_3-K_8m_4+K_9m_5,\quad P_1=K_3m_3-K_4m_1-C_5m_5,$$

$$P_2=m_4K_8-m_5K_9-m_6C_6-K_5m_1-K_6m_2-K_7m_3,$$